

Regular paper

## PM Synchronous Motor Control Strategies With Their Neural Network Regression Functions

*This paper proposes Surface Permanent Magnet Synchronous Motor (SPMSM) Control Strategies with Their Neural Network Regression Functions. Because the torque – angle control provides a wide variety of control choices in the PMSM drive system. Vector control of PMSM allows for the implementation of several choices of control strategies while control over torque is retained. Each of these control strategies are described and analyzed in this paper. All motor characteristics for all control techniques are introduced in the form of comparisons with such corresponding ones at rated conditions. The required terminal voltage to drive the motor at any prescribed technique is predicted. Then a brief description about Artificial Neural Network ANN; is illustrated to be used for predicting the required voltage to drive the motor at the desired control techniques for set of relations at various frequencies values under the base one. This is done to use the ability of neural network for interpolation with suitable number of layers and neurons. Finally, algebraic equations for each neural network case are presented to be used without the need of turning the neural models at each time.*

**Keywords:** Permanent magnet, Synchronous motor, Control Strategies, Neural Network and Matlab.

### 1. Introduction

Among the ac drives, permanent magnet synchronous machine (PMSM) drives have been increasingly applied in a wide variety of industrial applications. The reason comes from the advantages of PMSM: high power density and efficiency, high torque to inertia ratio, and high reliability. Recently, the continuous cost reduction of magnetic materials with high energy density and coercivity (e.g., samarium cobalt and neodymium-boron iron) makes the ac drives based on PMSM more attractive and competitive. In the high performance applications, the PMSM drives are ready to meet sophisticated requirements such as fast dynamic response, high power factor and wide operating speed range. This has opened up new possibilities for large-scale application of PMSM. Consequently, a continuous increase in the use of PMSM drives will surely be witnessed in the near future [1 - 3]. Sebastian and Slemmon [4] investigated the maximum torque per ampere (MTPA) operation of PMSM up to a break-point speed with optimum alignment of the stator and magnet field. Operation at higher speeds with reduced torque was achieved by the adjustment of current angle to reduce the effective magnet flux, i.e., the equivalent of field weakening. Dhaoui and Mohan researched a current-regulated flux-weakening method by introducing a negative current component to create direct-axis flux in opposition to that of the rotor flux by magnets, resulting in a reduced air-gap flux. This armature reaction effect was used to extend the operating speed range of PMSM and relieve the current regulator from saturation that is subject to occurring at high speeds [5]. Similarly, not only a current vector control to expand the operating limits under the constant inverter capacity but also the improvement by the feed-forward decoupling compensation were proposed in [6, 7] respectively by Morimoto et al. In these flux-weakening schemes, the demagnetizing current command was calculated based on the mathematical model of the PM motor and, consequently, the performance of the PMSM drive system was strongly dependent on the motor parameters and sensitive to operating conditions. Sozer and Torrey [8] presented an approach for adaptive control of the surface mounted PM motor over its entire speed range. The adaptive flux-weakening scheme was able to determine the right amount of direct-axis current without knowing the load torque and inverter parameters. C. Mademlis, and N. Margaris [9], presented an efficiency optimization method for vector-controlled interior permanent-magnet synchronous motor drive. Based on theoretical analysis, a loss minimization condition that determines

<sup>1</sup> Corresponding author: Adel El Shahat  
Department of Electrical and Computer Engineering, Ohio State University, USA. E-mail: [adel.elshahat@ieee.org](mailto:adel.elshahat@ieee.org),

<sup>2</sup> Department of Electrical Power and Machines Engineering, Zagazig University, Egypt. E.mail: [prof.hamed\\_elshevy@yahoo.com](mailto:prof.hamed_elshevy@yahoo.com)

the optimal q-axis component of the armature current was derived. Selected experimental results were presented to validate the effectiveness of the proposed control method.

Jian-Xin, Panda, Ya-Jun, Tong Heng, and Lam, B. H. [10] applied a modular control approach to a permanent-magnet synchronous motor (PMSM) speed control. Based on the functioning of the individual module, the modular approach enabled the powerfully intelligent and robust control modules to easily replace any existing module which did not perform well, meanwhile retaining other existing modules which were still effective. Using of ANN (Artificial Neural Network) in the field of electric machines especially with PM Synchronous Machine (PMSM) is not strange, like in the followed examples. Distinct advantages of the PMSM include low torque ripple, self commutation over a wider speed range, more efficient use of the volume of the machine and the ease with which it can be controlled [12]. But, there are some difficulties when operating with them, to overcome these difficulties, the artificial neural network (ANN) techniques of learning and control provide a natural framework for the design of online controllers for drive systems having unknown or uncertain dynamics [14]. The ability of the ANN to approximate nonlinear functions is the most significant. With the potential to shorten and generalize the model identification task and control scheme configuration, neural networks are extensively exploited in many control applications. Nowadays, in the ANN based control area, many researchers have been trying to develop efficient on-line adaptive learning algorithms for real-time implementation [13, 14-22]. Among them, Dynamic back-propagation (DBP) has gained a great attention [14], in which the neural network error gradient is evaluated on-line. In order to evaluate the gradient, with respect to the system output error between desired output and actual output, an identifier network has also been developed besides the controller network in most of the references. This scheme successfully utilizes back propagation of the system output error for the gradient evaluation, and extends the traditional static BP to a dynamic learning method in performing real-time identification and control.

The torque – angle control provides a wide variety of control choices in the PMSM drive system. Vector control of PMSM allows for the implementation of several choices of control strategies while control over torque is retained. Some key control strategies for the lower than base speed operating range are the following [11]:

- (a) Zero D-Axis Current (ZDAC)
- (b) Maximum Torque per Unit Current (MTPC)
- (c) Constant Mutual Flux Linkages (CMFL)
- (d) Unity Power Factor (UPF)

Each of these control strategies are described and analyzed in this paper. The deriving of the q and d-axis current commands as a function of torque and speed is described in each case. All motor characteristics for all control techniques are introduced in the form of comparisons with such corresponding ones at rated conditions. The required terminal voltage to drive the motor at any prescribed technique is predicted. Then a brief description about Artificial Neural Network ANN; is illustrated to be used for predicting the required voltage to drive the motor at the desired control techniques for set of relations at various frequencies values under the base one. By using ANN capabilities to deduce algebraic equations for each technique to make it easier for user to predict the required voltage to drive the motor at this certain technique with prescribed electromagnetic torque and desired frequency without training the network at each time.

## **2. Zero d-axis Current Control Strategy (ZDAC)**

The torque angle is defined as the angle between the q-axis current and the d-axis in the rotor reference frame. This angle is maintained at 90 degrees in the case of the ZDAC control strategy. The ZDAC control strategy is the most widely utilized control strategy by the industry. The d-axis current is effectively maintained at zero in this control strategy. The main advantage of this control strategy is that it simplifies the torque control mechanism by linearizing the relationship between torque and current. This means that a linear current controller results in linear control over torque as well. In dc motors the current and magnet fields are always maintained at an angle of 90 degrees. Therefore, the ZDAC control strategy makes a PMSM operate in a similar way to the dc motor. This makes the ZDAC control strategy very attractive for industrial designers who are used to operating dc motor drives. The following relationships hold for the ZDAC control strategy [11]:

$$T_e = \frac{3}{2} \frac{P}{2} \lambda_{af} I_q = \frac{3}{2} \frac{P}{2} \lambda_{af} I_s = 0.75 P \lambda_{af} I_s \quad (1)$$

where  $I_s$  is the phase magnitude, and

$$I_q = I_s \quad (2)$$

$$I_d = 0 \quad (3)$$

The air gap flux linkages can be described as

$$\lambda_m = (\lambda_{af}^2 + L_q^2 I_s^2)^{\frac{1}{2}} \quad (4)$$

The q and d axes voltages, in steady state, are

$$V_q = R_s I_s + \omega_r \lambda_{af} \quad (5)$$

$$V_d = -\omega_r L_q I_s \quad (6)$$

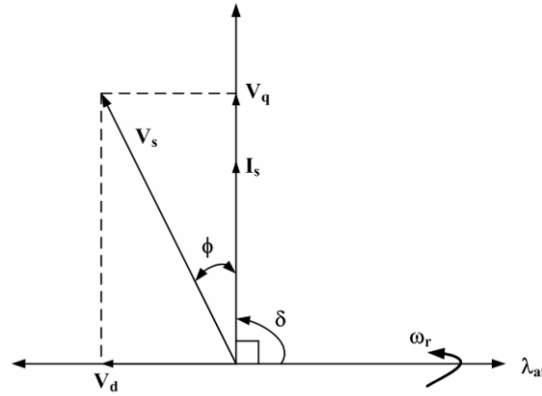


Fig. 1: Constant Torque Angle Control

It is notified that; the rate of change of currents is zero in the rotor reference frames, because the currents are constant in steady state. The magnitude of the voltage phasor is given by

$$V_s = \sqrt{V_q^2 + V_d^2} \quad (7)$$

From the phasor diagram in figure 1 and the axis voltages, power factor is obtained as

$$\cos \phi = \frac{V_q}{V_s} = \frac{V_q}{\sqrt{V_q^2 + V_d^2}} \quad (8)$$

This equation implies that the power factor deteriorates with increasing rotor speed as well as with increasing stator current. The ZDAC control strategy is the only control strategy that enforces zero d-axis current. This is one of the disadvantages of this control strategy as compared to the other control strategies. A non-zero d-axis current has the advantage of reducing the flux linkages in the d-axis by countering the magnet flux linkages. This serves to generate additional torque for inset and interior PMSM, and also reduces the air gap flux linkages. The following figures present comparisons between the surface permanent magnet motor characteristics at this control strategy with such ones at rated conditions. Then the required voltage to drive the motor at its rated frequency is presented. Finally, set of required voltages to drive the motor with this control strategy at various frequencies under rated one; which will consider being the learning data in the neural model in the next section.

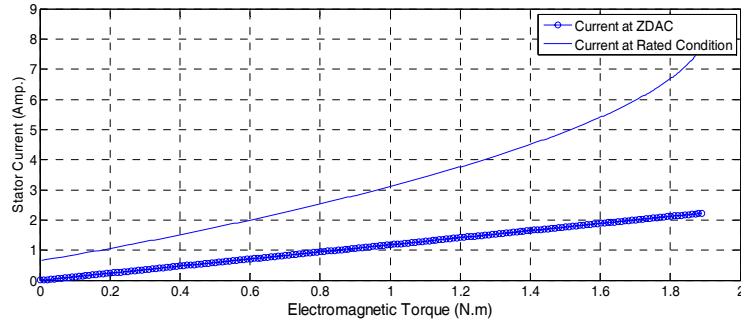


Fig. 2: Current Comparison at ZADC and rated conditions

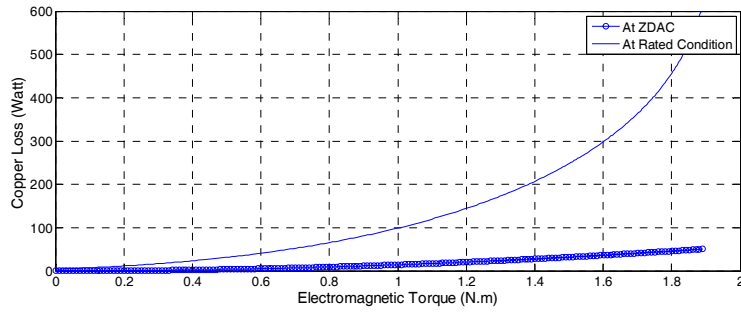


Fig. 3: Copper Loss Comparison at ZADC and rated conditions

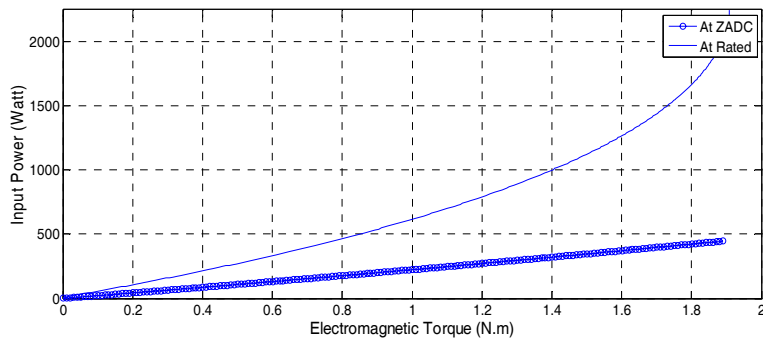


Fig. 4: Input Power Comparison at ZADC and rated conditions

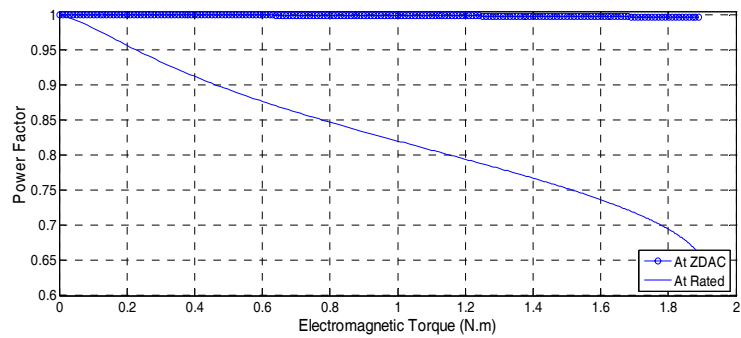


Fig. 5: Power Factor Comparison at ZADC and rated conditions.

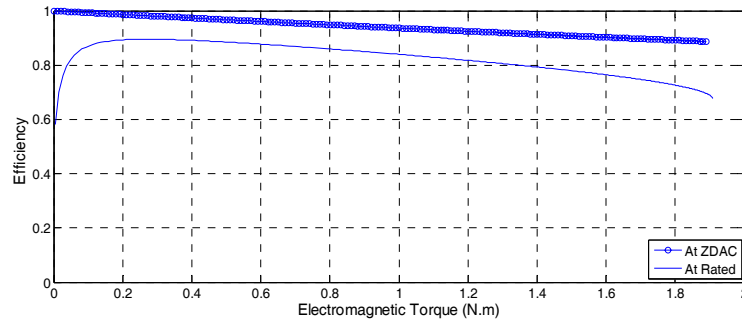


Fig. 6: Efficiency Comparison at ZADC and rated conditions

From all previous figures; it is clear that all performance characteristics are improved when proposing this technique as shown. Also, the required voltage at rated frequency to drive the motor at this control type is presented.

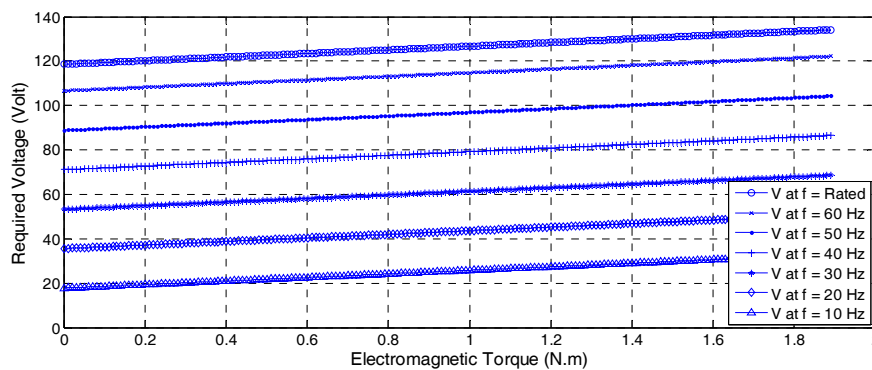


Fig. 7: Required Voltage to drive the motor with ZADC at Various Frequencies

The last set of relations introduced in figure 7 will be used in the next sections as training or learning data in the neural network model proposed there.

### 3. Artificial Neural Networks (ANNs) Technique

#### A. Introduction

An ANN consists of very simple and highly interconnected processors called neurons. The neurons are connected to each other by weighted links over which signals can pass. Each neuron receives multiple inputs from other neurons in proportion to their connection weights and generates a single output which may propagate to several other neurons [25]. Among the various kinds of ANNs that exist, the Back-propagation learning algorithm has become the most popular used method in engineering application. It can be applied to any feed-forward network with differentiable activation functions [26], and it is the type of network used in this paper.

#### B. Fundamentals of Neural Network

The ANN modeling is carried out in two steps; the first step is to train the network, whereas the second step is to test the network with data, which were not used for training. It is important that all the information the network needs to learn is supplied to the network as a data set. When each pattern is read, the network uses the input data to produce an output, which is then compared to the training pattern. If there is a difference, the connection weights are altered in such a direction that the error is decreased. After the network has run through all the input patterns, if the error is still greater than the maximum desired tolerance, the ANN runs through all the input patterns repeatedly until all the errors are within the required tolerance [27], [28].

### **C. Data Collection, Analysis and Processing**

The quality, availability, reliability, repeatability, and relevance of the data used to develop and run the system is critical to its success. Data processing starts from the data collections and analysis followed by pre-processing and then feeds to the neural network.

### **D. Network Structure Design**

Though theoretically there exists a network that can simulate a problem to any accuracy, there is no easy way to find it. To define an exact network architecture such as how many hidden layers should be used, how many units should there be within a hidden layer for a certain problem is a painful job.

#### **1) Number of Hidden Layers**

Because networks with two hidden layers can represent functions with any kind of shapes, there is no theoretical reason to use networks with more than two hidden layers. In general, it is strongly recommended that one hidden layer be the first choice for any feed-forward network design [25-28].

#### **2) Number of Hidden Units (node)**

Another important issue in designing a network is how many units to place in each layer. Using too few units can fail to detect the signals fully in a complicated data set, leading to under fitting. Using too many units will increase the training time, perhaps so much that it becomes impossible to train it adequately in a reasonable period of time. The best number of hidden units depends on many factors – the numbers of input and output units, the number of training cases, the amount of noise in the targets, the complexity of the error function, the network architecture, and the training algorithm. The best approach to find the optimal number of hidden units is trial and error.

#### **3) Initializing Back-Propagation feed-forward network**

Back-propagation is the most commonly used method for training multi-layer feed-forward networks. For most networks, the learning process is based on a suitable error function, which is then minimized with respect to the weights and bias. The algorithm for evaluating the derivative of the error function is known as back-propagation, because it propagates the errors backward through the network.

#### **4) Training the network**

Training occurs according to any training function as previous and we must decide the training parameters with their default values: The order used for training is for example

`[net, tr] = train (net, pn, tn)`

where pn, tn is the input and output which are normalized

#### **5) Network simulation**

To obtain the output of the network, we must simulate it the order, which can be used, is `an = sim (net, pn)`; where `an` is the network but normalized so if we want to un-normalize it we use this order `a = poststd (an, meant, stdt)`. To Performs a linear regression between the network response the target, and computes the correlation coefficient use the order `(R value between the network response and the target)`. `[m, b, r] = postreg (a, t)` [Matlab\ toolbox]; where `a, t` are the network output and desired or actual output and returns, `M` - Slope of the linear regression; `B` - Y intercept of the linear regression; `R` - Regression R-value. `R=1` means perfect correlation.

#### **6) Weights and Bias**

The weights and bias, can be obtained from training data by the orders; `Net.iw {1, 1}`...for the weight from input layer to hidden layer; `Net. {b1}` .....bias to a hidden layer  
`Net.lw {2, 1}`...for the weight from hidden layer to output layer; `Net. {b2}`... bias to output layer from a hidden layer

#### **7) Testing the network**

At first the data for testing mainly the input and the output from the network is prepared and then is compared with the desired or actual output to test the ability of the network by using the same initialized network.

[p1n, meanp1, stdp1, t1n, meant1, stdt1] = prestd (p1, t1)  
 net = train (net, p1n) ; an1 = sim (net, p1); [a1] = poststd (an1, meant1, stdt1); [m, b, r]=postreg (a1, t1)  
 where: p1, t1 are testing data, an1: is normalized output, a1: un- normalized output

**8) Derived mathematical equations**

Finally mathematical equations can be derived [29], in order to be used in future to calculate the output from the input data without needing to construct a neural network by using the weights and bias according to activation and transfer functions as when using {logsig 'purelin} as in this paper, the next sequences have to be followed

- 1- Normalize the input data as shown previous .
- 2- Calculate sum of  $x_i * w_{i,j} + b_{i,j} = h_i$  for each node in hidden layer  
 where:  $x_i$ : is the input variable,  $h_i$ : is a hidden layer input from input layer  $w_{i,j}$ ,  $b_{i,j}$  are obtained before,  $Net.iw\{1,1\}$   $Net.b\{1\}$
- 3- Calculate the output from each node in hidden layer to output layer ( $F_i$ ) according to transfer function here is logsig so  $F_i = 1/(1+exp(-h_i))$
- 4- Calculate the sum of output from hidden layer to output layer  $h_i = F_i * Net.lw\{2,1\} + Net.b\{2\}$
- 5- Calculate the required output according to transfer fun. here is purelin [Matlab/toolbox] so output ( $y_i$ ) =  $h_i$  according to number of the required outputs
- 6- Un normalized  $y$  to obtain the output =  $y * stdt + meant$  ...to obtain the actual values

**4. Ann Zero d-axis Current Control Model with Its Equation**

Using the neural network technique described before in implementing a neural model to connect between three variables that: entering the desired frequency and electromagnetic torque range as input to generate the required voltage to drive the motor at this technique for this range of frequencies under the base one. This model tries to make more generalization for these relations in figure 7 to make benefits from the ability of neural network of interpolation between points and also curves. Finally, the algebraic equation is deduced to use it without training the neural unit in each time. One can ask a question that; why the curve fitting facility could not be used for more simplicity? The answer is this could be used for single curve but neural equation given more globalization view. Also, this model has a suitable number of layers and neurons in each layer on the basis prescribed before. This model is summarized in figure 8.

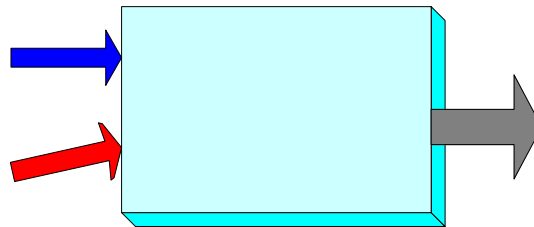


Fig. 8: ZADC Neural Model

This neural model has the ability to deal with all curves in figure 7 as surface or mapping face as shown in figure 9, due to this technique advantages especially its ability to interpolation between points with each other and also curves.

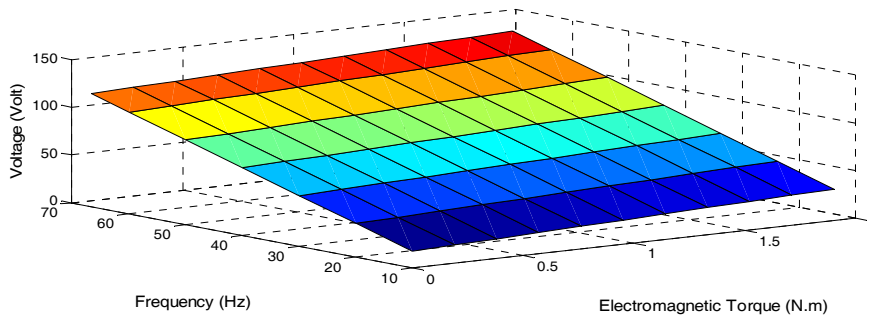


Fig. 9: The relation among Req. Voltage, frequency, and Torque

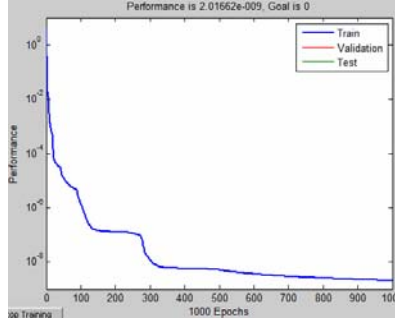


Fig. 10: Training result for Neural Model

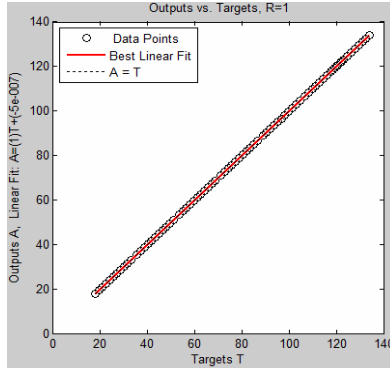


Fig. 11: Comparison of actual and ANN-predicted values for Voltage

$$T_{en} = (T_e - 0.9510) / (0.6048) \tag{9}$$

$$f_n = (f - 39.5238) / (19.4344) \tag{10}$$

Equations (9), and (10) present the normalized inputs for electromagnetic torque and frequency, and the following equations lead to the required voltage derived equation.

$$E1 = -0.1377 T_{en} + 0.1827 f_n + 0.2467 \tag{11}$$

$$F1 = 1 / (1 + \exp(-E1))$$

$$E2 = -0.1165 T_{en} + -0.6995 f_n + 2.3064 \tag{12}$$

$$F2 = 1 / (1 + \exp(-E2))$$

$$E3 = 4.8308 T_{en} + -5.6780 f_n + 3.3650 \tag{13}$$

$$F3 = 1 / (1 + \exp(-E3))$$

$$E4 = -0.0149 T_{en} + -0.1676 f_n + -0.3754 \tag{14}$$

$$F4 = 1 / (1 + \exp(-E4))$$

$$V_{sn} = -1.2914 F1 + -0.8953 F2 + 0.0002 F3 + -24.6252 F4 + 11.5669 \tag{15}$$

The un- normalized out puts

$$V_s = 34.9537 V_{sn} + 77.9837 \tag{16}$$

### 5. Max. Torque per Unit Current Control Strategy (MTPC)

The MTPC control strategy is the most widely studied control strategy. Application of this control strategy results in the production of maximum possible torque at any given current. This control strategy minimizes current for a given torque. Consequently, copper losses are minimized in the process. For the types of PMSM that do not exhibit magnetic saliency the MTPC and ZDAC control strategies are the same. The MTPC control strategy results in maximum utilization of the drive as far as current if concerned [11]. This is due to the fact that more torque is delivered for unit current as compared to other techniques. This means the ZDAC control strategy presented in previous section

with its neural network model are the same as for MTPC control strategy for SPMSM which we deal with it in this study. So, as affirmative figure on this idea, figure 12 shows the torque per ampere ratio from ZDAC control i.e. MTPC in comparable with such on at rated conditions.

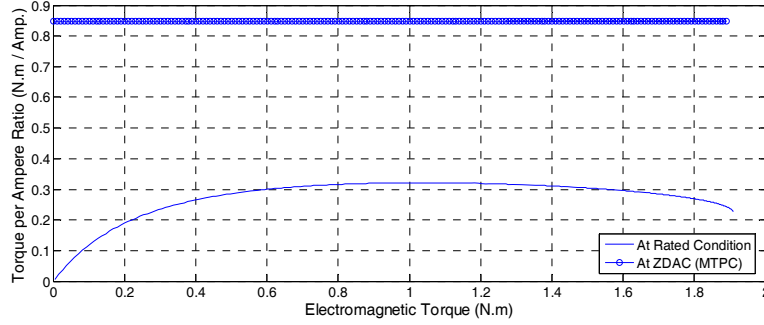


Fig. 12: Torque per Amp. Ratio Comparison at ZADC and rated conditions

The maximum torque per ampere technique for (IPMSM) Interior Permanent Magnet Synchronous Motor is also introduced with its neural network model before by the same authors [23, 24].

### 6. Unity Power Factor Control Strategy (UPF)

Unity – power – factor (UPF) control implies that the VA rating of the inverter is fully utilized for real power input to the PMSM [11]. UPF control is enforced by controlling the torque angle as a function of motor variables. The performance equations in this mode of operation are derived and given below.

$$T_e = \frac{3}{2} \frac{P}{2} \lambda_{af} I_s \sin \alpha = 0.75 P \lambda_{af} I_s \tag{17}$$

$$v_q = R_s I_s \sin \alpha + \omega_r L_d I_s \cos \alpha + \omega_r \lambda_{af} \tag{18}$$

$$v_d = R_s I_s \cos \alpha - \omega_r L_q I_s \sin \alpha \tag{19}$$

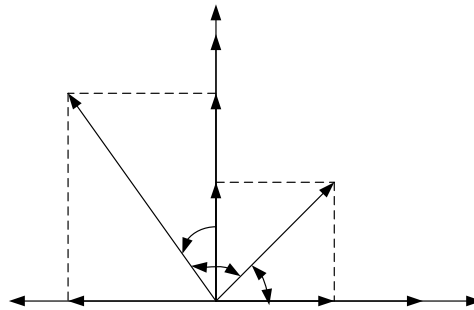


Fig. 13: Phasor diagram of the PM synchronous machine

The angle between d axis and the resultant voltage  $V_s$  is

$$\tan(\alpha + \phi) = \frac{v_q}{v_d} \tag{20}$$

Since the power factor angle has to be zero in this control type

$$\phi = 0 \tag{21}$$

which gives the following relationship for the torque angle:

$$\tan \alpha = \frac{v_q}{v_d} \tag{22}$$

Upon substitution of equations above into (22)

$$\tan \alpha = \frac{R_s I_s \sin \alpha + \omega_r L_d I_s \cos \alpha + \omega_r \lambda_{af}}{R_s I_s \cos \alpha - \omega_r L_q I_s \sin \alpha} = \frac{R_s \sin \alpha + \omega_r L_d \cos \alpha + \frac{\omega_r \lambda_{af}}{I_s}}{R_s \cos \alpha - \omega_r L_q \sin \alpha} = \frac{\sin \alpha}{\cos \alpha} \quad (23)$$

$$R_s \cos \alpha \sin \alpha - \omega_r L_q \sin^2 \alpha = R_s \sin \alpha \cos \alpha + \omega_r L_d \cos^2 \alpha + \cos \alpha \frac{\omega_r \lambda_{af}}{I_s}$$

For surface PM Synchronous Motor  $L_d = L_q = L_s$

$$0 = \omega_r L_q (\sin^2 \alpha + \cos^2 \alpha) + \cos \alpha \frac{\omega_r \lambda_{af}}{I_s} \quad (24)$$

$$\cos \alpha = -\frac{L_s I_s}{\lambda_{af}} \Rightarrow \alpha = \cos^{-1} \left( -\frac{L_s I_s}{\lambda_{af}} \right) \quad (25)$$

The following figures present comparisons between the most important characteristics at this control technique with such ones at rated conditions. This is done to imply the performance improvement due to this technique.

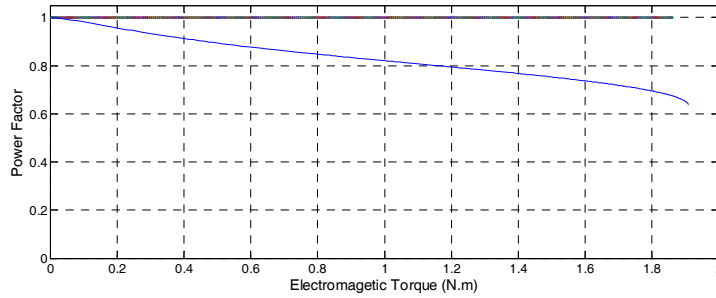


Fig. 14: Power Factor Comparison at UPF and rated conditions

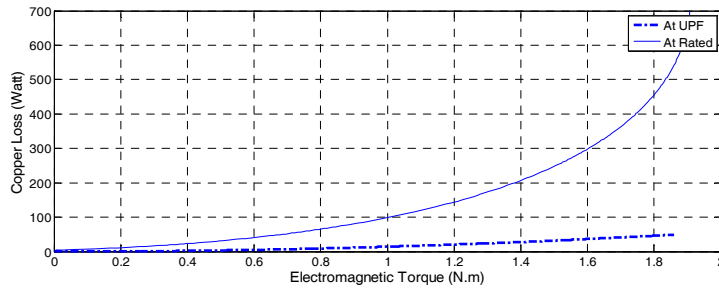


Fig. 15: Copper Loss Comparison at UPF and rated conditions

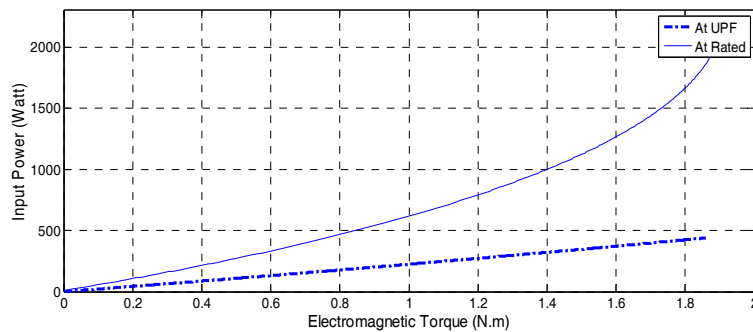


Fig. 16: Input Power Comparison at UPF and rated conditions

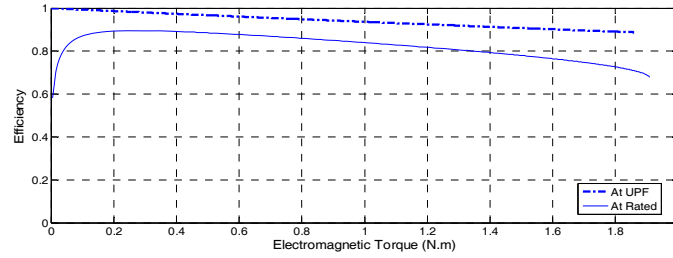


Fig. 17: Efficiency Comparison at UPF and rated conditions

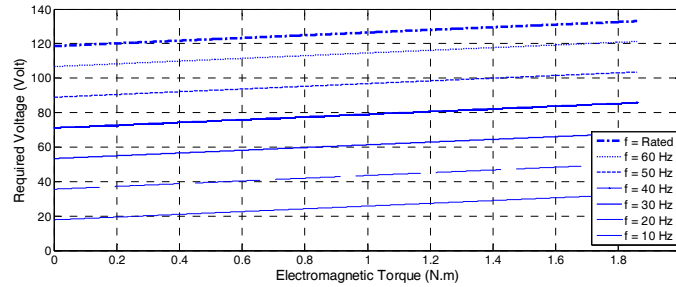


Fig. 18: Required Voltage at UPF with Torque for variable frequency

From all previous figures; it is clear that all performance characteristics are improved when proposing this technique as shown. Also, the required voltage at various frequencies to drive the motor at this control type is presented in fig. 18. These relations introduced in figure 18 will be used in the next section as training or learning data in the neural network model proposed there.

### 7. Unity Power Factor Control Strategy Neural Model

Using the neural network technique described before in implementing a neural model to connect between three variables that: entering the desired frequency and electromagnetic torque range as input to generate the required voltage to drive the motor at this technique for this range of frequencies under the base one. This model uses the relations in figure 18 as training or learning data. Then its algebraic equation is deduced to use it without training the neural unit in each time. This model has a suitable number of layers and neurons in each layer on the basis prescribed before. This model is summarized as in figure 8 for the same number of layers and neuron.

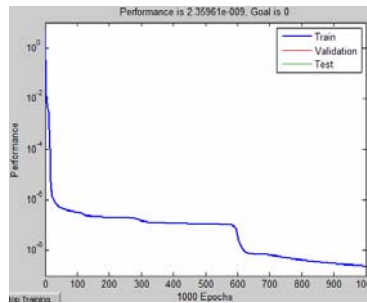


Fig. 19: Training result for Neural Model

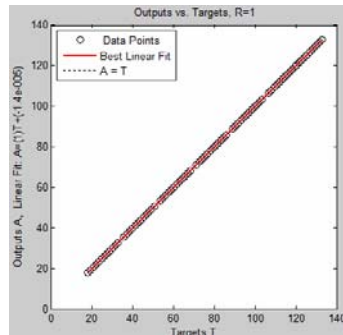


Fig. 20: Comparison of actual and ANN-predicted values for Voltage

$$T_{en} = (T_e - 0.9327)/(0.5875) \tag{26}$$

$$f_n = (f - 39.5238)/(19.4237) \tag{27}$$

Equations (26), and (27) present the normalized inputs for electromagnetic torque and frequency, and the following equations lead to the required voltage derived equation.

$$E1 = 0.0650T_{en} + 0.4525f_n + -1.8242 \tag{28}$$

$$F1 = 1 / (1 + \exp(-E1))$$

$$E2 = 0.2508T_{en} + -0.1741f_n + -0.2329 \tag{29}$$

$$F2 = 1 / (1 + \exp(-E2))$$

$$E3 = -0.0412T_{en} + -0.2417f_n + -0.8434 \tag{30}$$

$$F3 = 1 / (1 + \exp(-E3))$$

$$E4 = 4.7437T_{en} + 1.4749f_n + 7.3055 \tag{31}$$

$$F4 = 1 / (1 + \exp(-E4))$$

$$V_{sn} = 4.1053F1 + -0.4342F2 + -14.7606F3 + -0.0010F4 + 4.0633 \tag{32}$$

The un- normalized out puts

$$V_s = 34.7999V_{sn} + 77.6676 \tag{33}$$

### 8. Constant Mutual Flux Linkages Control Strategy (CMFL)

In this control strategy, the resultant flux linkage of the stator q and d axes and rotor, known as the mutual flux linkage, is maintained constant, most usually at a value equal to the rotor flux linkage,  $\lambda_{af}$ . Its main advantage is that, by the limiting of the mutual flux linkages, the stator voltage requirement is kept comparably low. In addition, varying the mutual flux linkages provides a simple and straightforward flux-weakening for operation at speeds higher than the base speed. Hence, mutual flux linkages control is one of the powerful techniques useful in the entire speed range, as against other schemes that are limited to operation lower than the base speed only. The mutual flux linkage is expressed as follows [11]:

$$\lambda_m = \sqrt{(\lambda_{af} + L_d I_d)^2 + (L_q I_q)^2} \tag{34}$$

and, for example, equating it to the rotor flux linkages as

$$\lambda_m = \lambda_{af} \tag{35}$$

and substituting for the direct and quadrature axis currents in terms of the stator current phasor.

$$\lambda_{af}^2 = (\lambda_{af} + L_d I_d)^2 + (L_q I_q)^2 \tag{36}$$

$$\lambda_{af}^2 = \lambda_{af}^2 + 2\lambda_{af} L_d I_d + (L_d I_d)^2 + (L_q I_q)^2$$

$$0 = 2\lambda_{af} L_d I_s \cos \alpha + L_d^2 I_s^2 \cos^2 \alpha + L_q^2 I_s^2 \sin^2 \alpha$$

For surface PM Synchronous Motor  $L_d = L_q = L_s$

$$0 = 2\lambda_{af} \cos \alpha + L_s I_s (\cos^2 \alpha + \sin^2 \alpha)$$

$$\cos \alpha = -\frac{L_s I_s}{2\lambda_{af}} \Rightarrow \alpha = \cos^{-1}\left(-\frac{L_s I_s}{2\lambda_{af}}\right) \tag{37}$$

The following figures present comparisons between the various characteristics at this control technique with such ones at rated conditions. This is to show the performance improvement due to this technique.

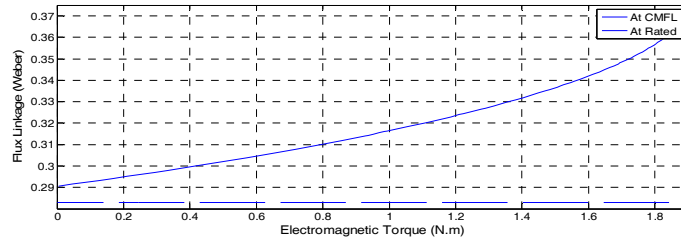


Fig. 21: Flux Linkage Comparison at CMFL and rated conditions

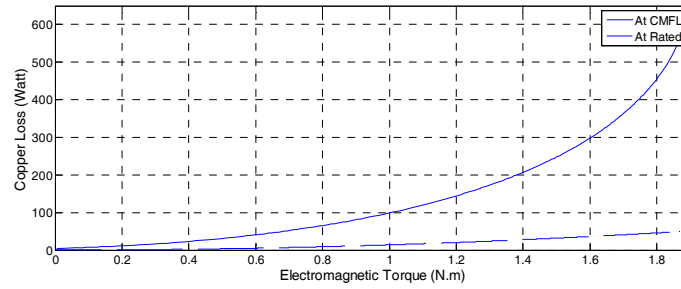


Fig. 22: Copper Loss Comparison at CMFL and rated conditions

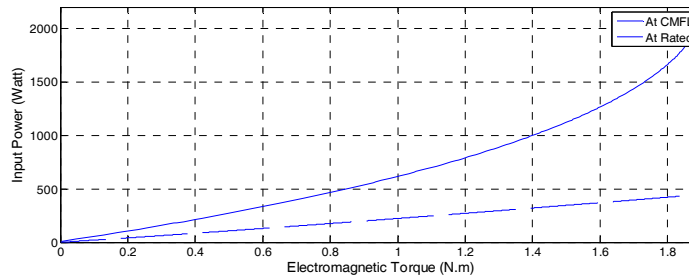


Fig. 23: Input Power Comparison at CMFL and rated conditions

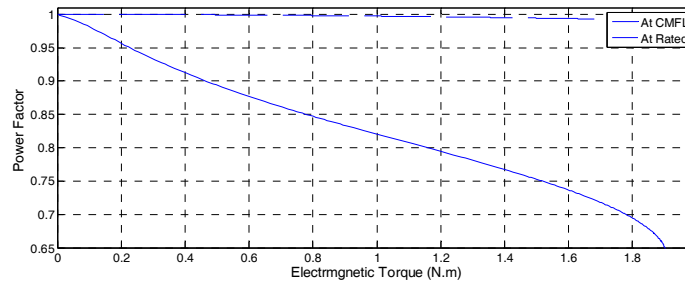


Fig. 24: Power Factor Comparison at CMFL and rated conditions

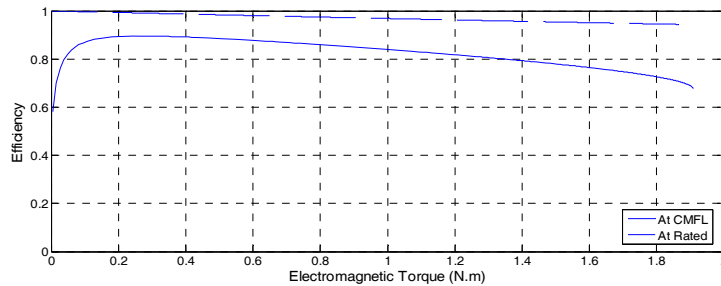


Fig. 25: Efficiency Comparison at CMFL and rated conditions

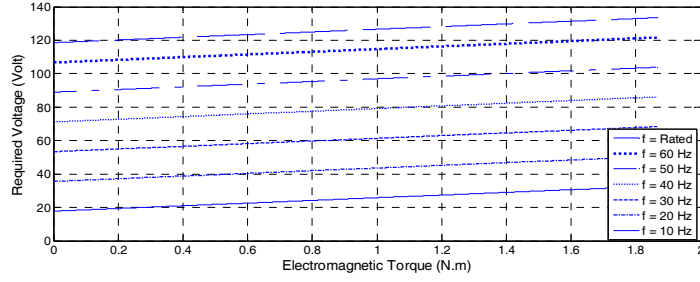


Fig. 26: Required Voltage at CMFL with Torque for variable frequency

**9. Constant Mutual Flux Linkages Control Neural Model**

Using the neural network technique described before in implementing a neural model to connect between three variables that: entering the desired frequency and electromagnetic torque range as input to generate the required voltage to drive the motor at this technique for this range of frequencies under the base one. This model uses the relations in figure 26 as training or learning data. Then its algebraic equation is deduced to use it without training the neural unit in each time. This model has a suitable number of layers and neurons in each layer on the basis prescribed before. This model is summarized in figure 8 also.

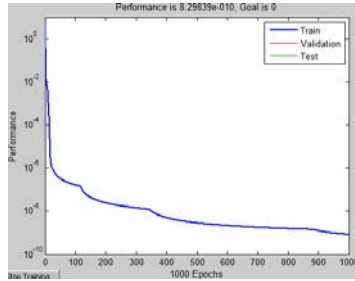


Fig. 27: Training result for Neural Model

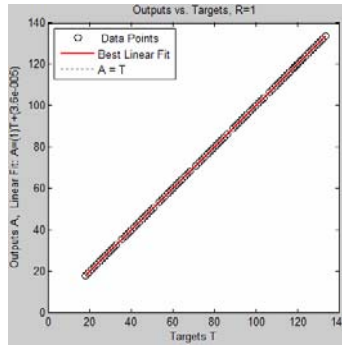


Fig. 28: Comparison of actual and ANN-predicted values for Voltage

$$T_{en} = (T_e - 0.9342)/(0.5891) \tag{38}$$

$$f_n = (f - 39.5238)/(19.4237) \tag{39}$$

Equations (38), and (39) present the normalized inputs for electromagnetic torque and frequency, and the following equations lead to the required voltage derived equation.

$$E1 = 0.0421T_{en} + 0.3084f_n + - 1.4514 \tag{40}$$

$$F1 = 1 / (1 + \exp(- E1))$$

$$E2 = 7.2669T_{en} + - 9.3254f_n + - 5.8556 \tag{41}$$

$$F2 = 1 / (1 + \exp(- E2))$$

$$E3 = -0.0363T_{en} + -0.2658f_n + -1.2116 \quad (42)$$

$$F3 = 1 / (1 + \exp(-E3))$$

$$E4 = 4.9406T_{en} + 3.4972f_n + 11.0087 \quad (43)$$

$$F4 = 1 / (1 + \exp(-E4))$$

$$V_{sn} = 8.9681F1 + -0.00002F2 + -12.0351F3 + -0.00001F4 + 1.0591 \quad (44)$$

The un- normalized out puts

$$V_s = 34.8587V_{sn} + 77.7624 \quad (45)$$

## 10. Conclusions

Control Strategies of Surface Permanent Magnet Synchronous Motor (SPMSM) are presented in this paper. Moreover, Neural Network Models with Algebraic Regression Functions for each control technique are deduced. These control strategies are depending on the torque – angle because of a wide variety of control choices in the PMSM drive system, and the allowance for the implementation. Each of these control strategies are described and analyzed in this paper. All motor characteristics for all control techniques are introduced in the form of comparisons with such corresponding ones at rated conditions to show the deal of performance improvement. The required terminal voltage to drive the motor at any desired control technique is deduced for any frequency values under the base speed. This study affirms on the advantages and disadvantages of these various techniques as the following: The ZDAC control strategy is the most widely utilized control strategy by the industry. The d-axis current is effectively maintained at zero in this control strategy. The main advantage of this control strategy is that it simplifies the torque control mechanism by linearizing the relationship between torque and current. The ZDAC control strategy is the only control strategy that enforces zero d-axis current. This is one of the disadvantages of this control strategy as compared to the other control strategies. A non-zero d-axis current has the advantage of reducing the flux linkages in the d-axis by countering the magnet flux linkages. This serves to generate additional torque for inset and interior PMSM, and also reduces the air gap flux linkages. Then, the MTPC control strategy is the most widely studied control strategy. For the types of PMSM that do not exhibit magnetic saliency the MTPC and ZDAC control strategies are the same. The MTPC control strategy results in maximum utilization of the drive as far as current if concerned. Later, Unity – power – factor (UPF) control implies that the VA rating of the inverter is fully utilized for real power input to the PMSM. Finally, the main advantage of CMFL is that, by the limiting of the mutual flux linkages, the stator voltage requirement is kept comparably low. In addition, varying the mutual flux linkages provides a simple and straightforward flux-weakening for operation at speeds higher than the base speed. Hence, mutual flux linkages control is one of the powerful techniques useful in the entire speed range, as against other schemes that are limited to operation lower than the base speed only. For all neural models the inputs are the desired frequency and electromagnetic torque range as to generate the required voltage to drive the motor at any desired technique with this range of frequencies under the base one. This model tries to make more generalization for these voltages relations to make benefits from the ability of neural network of interpolation between points and also curves. The algebraic equation is deduced to use it without training the neural unit in each time. Also, this model has a suitable number of layers and neurons in each layer on the basis prescribed before. This neural model has the ability to deal with all curves as surface or mapping face, due to this technique advantages. All neural network units are the back propagation (BP) learning algorithm due to its benefits. The validity of these units comes from comparisons between techniques values obtained in MATLAB environment with corresponding from Neural Networks. Also, this technique will be used further in more complex systems.

## Appendix

SPMSM ratings and parameters:  $L_q = 0.0115$  H;  $L_d = 0.0115$  H;  $\lambda_{af} = 0.283$ ;  $P = 4$ ;  $R_s = 6.8 \Omega$ ;  $V_s = 200$  V;  $N_s = 2000$  rpm;  $B = 0.0005416$ ;  $J = 0.0000144$ ;  $T_d = 0.1698$

## References

- [1] B. K. Bose, "Power electronics and motion control—Technology status and recent trends," *IEEE Trans. Ind. Applicat.*, vol. 29, pp. 902–909, Sept./Oct., 1993.
- [2] W. Leonhard, "Adjustable speed ac drives," *Proceedings of IEEE*, vol. 76, pp. 455–471, April, 1988.
- [3] B. K. Bose, "Variable frequency drives—technology and applications," *Proc. ISIE 93(Budapest)*, June, 1993, pp. 1–18.
- [4] T. Sebastian and G. R. Slemon, "Operating limits of inverter-driven permanent magnet motor drives," *IEEE CH2272-3/86*, pp. 800–805, 1986.
- [5] R. Dhaouadi and N. Mohan, "Analysis of current-regulated voltage-source inverters for permanent magnet synchronous motor drives in normal and extended speed ranges," *IEEE Trans. Energy Conv.*, vol. 5, pp. 137–144, Mar. 1990.
- [6] S. Morimoto, M. Sanada and K. Takeda, "Wide-speed operation of interior permanent magnet synchronous motors with high-performance current regulator," *IEEE Trans. Ind. Applicat.*, vol. 30, pp. 920–926, July/Aug. 1994.
- [7] S. Morimoto, Y. Takeda, T. Hirasaka, and K. Taniguchi, "Expansion of operating limits for permanent magnet by current vector control considering inverter capacity," *IEEE Trans. Ind. Appl.*, vol. 26, pp. 866–871, Sept./Oct. 1990.
- [8] Y. Sozer and D. A. Torrey, "Adaptive Flux weakening control of permanent magnet synchronous motors," in *Conf. Rec. IEEE-IAS Annu. Meeting*, vol. 1, St. Louis, MO, 1998, pp. 475–482.
- [9] C. Mademlis and N. Margaris, "Loss minimization in vector-controlled interior permanent-magnet synchronous motor drives," *Industrial Electronics, IEEE Transactions on*, vol. 49, pp. 1344–1347, 2002.
- [10] X. Jian-Xin, S. K. Panda, P. Ya-Jun, L. Tong Heng, and B. H. Lam, "A modular control scheme for PMSM speed control with pulsating torque minimization," *Ind. Electronics, IEEE Transactions on*, vol. 51, pp. 526–536, 2004.
- [11] R. Krishnan, *Electric Motor Drives: Modeling, Analysis & Control*, Prentice Hall, 2006.
- [12] T. J. E. Miller, *Brushless Permanent Magnet and Reluctance Motor Drives*, Oxford, UK: Clarendon, 1989.
- [13] M. A. Rahman, M. A. Hoque, and, "On-line adaptive artificial neural network based vector control of permanent magnet synchronous motors," *IEEE Trans. On Energy Conversion*, vol. 13, Dec. 1998, pp. 311–318.
- [14] A. Rubaai, R. Koteru, M. D. Kankam, "A continually online-trained neural network controller for brushless dc motor drives", *IEEE Trans. On Industry Applications*, vol. 36, no. 2, 2000, pp. 475–483.
- [15] S. Weerasooriya and M. A. El-Sharkawi, "Identification and control of a dc motor using back-propagation neural networks", *IEEE Trans. On Energy Conversion*, Vol. 6, No. 4, 1991, pp.663–669.
- [16] S. Weerasooriya and M. A. El-Sharkawi, "Laboratory implementation of a neural network trajectory controller for a dc motor", *IEEE Trans. on Energy Conversion*, Vol. 8, Mar. 1993, pp.107–113.
- [17] M. A. Hoque, M. R. Zaman, and M. A. Rahman, "Artificial neural networks based controller for permanent magnet dc motor drives," in *IEEE/IAS Annual Meeting Record*, Orlando, FL, Oct. 1995, pp. 775–780.
- [18] A. Rubaai and R. Koteru, "Neural net-based robust controller design for brushless dc motor drives", *IEEE Trans. on Systems, Man, and Cybernetics*, Vol. 29, 3, Aug. 1999, pp.460–474.
- [19] A. Rubaai and R. Koteru, "Parallel computation of continually on-line trained neural networks for identification and control of induction motors", in *IEEE/IAS Annual Meeting Record*, Vol. 4, 1999, pp.2364–2371.
- [20] B. Burton and R. G. Harley, "Reducing the computational demands of continually online training artificial neural networks for system identification and control of fast processes", *IEEE Trans. on Neural Networks*, vol. 1, Mar. 1990, pp.4–27.
- [21] M. Elbuluk, T. Liu, I. Husain, "Neural network-based model reference adaptive systems for high performance motor drives and motion controls", in *Conf. Record, IEEE Ind. Appl. Conference*, 2000, vol. 2, pp. 959–965.
- [22] K. S. Narendra and K. Parthasarathy, "Gradient-methods for the optimization of dynamical systems containing neural networks," *IEEE Trans. on Neural Networks*, vol. 2, March 1991, pp.252–262.
- [23] A. El Shahat, H. El Shewy, "Neural Unit for PM Synchronous Machine Performance Improvement used for Renewable Energy", Paper Ref.: 910, Accepted in Global Conference on Renewable and Energy Efficiency for Desert Regions (GCREEDER2009), Amman, Jordan.
- [24] El Shahat, A and El Shewy, H, "Neural Unit for PM Synchronous Machine Performance Improvement used for Renewable Energy", Ref: 93, Accepted in The Third Ain Shams University International Conference on Environmental Engineering (Ascee- 3 ), April 14-16 2009, Cairo, Egypt.
- [25] TT Chow, Zhang GQ, Lin Z, Song CL. :Global optimization of absorption chiller system by genetic algorithm and neural network. *Energy Buildings* 2002;34:103–9.
- [26] SA Kalogirou "Applications of artificial neural networks in energy systems: a review," *Energy Convers Manage* 1999; 40:1073–87.
- [27] SA. Kalogirou "Applications of artificial neural networks for energy systems," *Appl Energy* 2000; 67:17–35.
- [28] SA. Kalogirou "Long-term performance prediction of forced circulation solar domestic water heating Systems using artificial neural networks," *Appl Energy* 2000; 66:63–74.
- [29] Arzu Sencan, Kemal A.Yakut, Soteris A.Kalogirou " Thermodynamic analysis of absorption systems using artificial neural network," *Renewable Energy*, Volume 31, issue 1, Jan. 2006, pages 29 – 43.